

# A *Chandra* X-ray observation of the globular cluster Terzan 1

E. M. Cackett<sup>1</sup>\*, R. Wijnands<sup>2</sup>, C. O. Heinke<sup>3,4</sup>, D. Pooley<sup>5,6</sup>, W. H. G. Lewin<sup>7</sup>, J. E. Grindlay<sup>8</sup>, P. D. Edmonds<sup>8</sup>, P. G. Jonker<sup>8,9</sup>, J. M. Miller<sup>10</sup>

<sup>1</sup> School of Physics and Astronomy, University of St. Andrews, KY16 9SS, Scotland, UK

<sup>2</sup> Astronomical Institute ‘Anton Pannekoek’, University of Amsterdam, Kruislaan 403, 1098 SJ, Amsterdam, the Netherlands

<sup>3</sup> Department of Physics and Astronomy, Northwestern University, 2145 Sheridan Road, Evanston, IL 60208, USA

<sup>4</sup> Lindheimer Postdoctoral Fellow

<sup>5</sup> Astronomy Department, UC Berkeley, 601 Campbell Hall, Berkeley, CA 94720-3411, USA

<sup>6</sup> Chandra Fellow

<sup>7</sup> Center for Space Research, Massachusetts Institute of Technology, 77 Massachusetts Avenue, Cambridge, MA 02139, USA

<sup>8</sup> Harvard-Smithsonian Center for Astrophysics, 60 Garden Street, Cambridge, MA 02138, USA

<sup>9</sup> SRON, National Institute for Space Research, Sorbonnelaan 2, 3584 CA Utrecht, the Netherlands

<sup>10</sup> University of Michigan, Department of Astronomy, 500 Church Street, Dennison 814, Ann Arbor, MI 48105

Received ; in original form

## ABSTRACT

We present a  $\sim$ 19 ks *Chandra* ACIS-S observation of the globular cluster Terzan 1. Fourteen sources are detected within 1 $'$ 4 of the cluster center with 2 of these sources predicted to be not associated with the cluster (background AGN or foreground objects). The neutron star X-ray transient, X1732–304, has previously been observed in outburst within this globular cluster with the outburst seen to last for at least 12 years. Here we find 4 sources that are consistent with the *ROSAT* position for this transient, but none of the sources are fully consistent with the position of a radio source detected with the VLA that is likely associated with the transient. The most likely candidate for the quiescent counterpart of the transient has a relatively soft spectrum and an unabsorbed 0.5–10 keV luminosity of  $2.6 \times 10^{32}$  ergs s $^{-1}$ , quite typical of other quiescent neutron stars. Assuming standard core cooling, from the quiescent flux of this source we predict long ( $> 400$  yr) quiescent episodes to allow the neutron star to cool. Alternatively, enhanced core cooling processes are needed to cool down the core. However, if we do not detect the quiescent counterpart of the transient this gives an unabsorbed 0.5–10 keV luminosity upper limit of  $8 \times 10^{31}$  ergs s $^{-1}$ . We also discuss other X-ray sources within the globular cluster. From the estimated stellar encounter rate of this cluster we find that the number of sources we detect is significantly higher than expected by the relationship of Pooley et al. (2003).

**Key words:** globular clusters: individual (Terzan 1) — stars: neutron — stars: individual (X 1732-304) — X-rays: binaries

## 1 INTRODUCTION

Neutron star X-ray transients form a subgroup of low-mass X-ray binaries. Although usually in a quiescent state with typical X-ray luminosities of  $10^{32}$  -  $10^{34}$  ergs s $^{-1}$ , occasionally these systems go into outburst where the luminosity increases to around  $10^{36}$  -  $10^{38}$  ergs s $^{-1}$ . These outbursts are attributed to a large increase in the mass accretion rate onto the neutron star. The X-ray spectra from these quiescent neutron star transients are usually dominated by a

soft component at around 1 keV, and in some cases an additional power-law component, dominating at energies above a few keV, is present. The most widely accepted model used to explain the soft, thermal X-ray emission of these transients in their quiescent states is that in which the emission is due to the cooling of the neutron star, which has been heated during the outbursts. In this case, the quiescent luminosity should depend on the time-averaged accretion rate (Brown et al. 1998; Campana et al. 1998). However, the X-ray emission from the cooling of the neutron star cannot directly explain the hard power-law tail and its origin is not well understood. Suggestions include resid-

\* emc14@st-andrews.ac.uk

ual accretion down to the magnetospheric radius, or pulsar shock emission (e.g., Stella et al. 1994; Campana et al. 1998; Campana & Stella 2000; Menou & McClintock 2001).

Many quiescent neutron stars and other quiescent low-mass X-ray binaries have been found in several globular clusters using the *Chandra* and *XMM-Newton* X-ray observations (see Heinke et al. 2003c; Pooley et al. 2003, and references therein). Galactic globular clusters provide an ideal location to study these types of sources - the distance to host clusters can usually be determined more accurately than for the Galactic quiescent X-ray binaries. The known distance and reddening allows accurate luminosities to be derived and removes the distance uncertainty from the quiescent properties. The high incidence of compact binaries in globular clusters is likely explained by the formation of such binaries via exchange encounters in the very dense environments present.

Terzan 1 (Terzan 1966) is a globular cluster at a distance of  $5.2 \pm 0.5$  kpc and a reddening of  $E(B - V) = 2.48 \pm 0.1$  (Ortolani et al. 1999). In 1980, the *Hakucho* satellite detected X-ray bursts from a source located in Terzan 1 (Makishima et al. 1981; Inoue et al. 1981). Several years later, the persistent source X1732-304 was detected within Terzan 1 with SL2-XRT onboard Spacelab 2 (Skinner et al. 1987) and *EXOSAT* (Warwick et al. 1988; Parmar et al. 1989). This is likely to be the same source as the bursting source detected previously by *Hakucho*. Subsequent X-ray observations with *ROSAT* (Johnston et al. 1995; Verbunt et al. 1995) detected the source with a similar luminosity, between a few times  $10^{35}$  ergs  $s^{-1}$  and  $\sim 10^{37}$  ergs  $s^{-1}$  (see Fig. 3 of Guainazzi et al. 1999). It is also assumed that X1732-304 is the source of hard X-rays detected with the SIGMA and ART-P telescopes (Borrel et al. 1996a,b; Pavlinsky et al. 1995). A possible radio counterpart of X1732-304 was observed with the VLA within the *ROSAT* error circles (Marti et al. 1998).

A *BeppeSAX* observation of X1732-304 in April 1999 discovered the source in a particularly low state with the X-ray intensity more than a factor of 300 lower than previous measurements (Guainazzi et al. 1999). A more recent short ( $\sim 3.6$  ks) *Chandra* HRC-I observation of Terzan 1 did not conclusively detect X1732-304 with a 0.5-10 keV luminosity upper limit of  $(0.5 - 1) \times 10^{33}$  ergs  $s^{-1}$  depending on the assumed spectral model (Wijnands, Heinke & Grindlay 2002). However, an additional X-ray source, CXOGLB J173545.6-302900, was detected by this observation.

In this paper we study the X-ray sources detected in a recent  $\sim 19$  ks *Chandra* ACIS-S observation of Terzan 1 and discuss possible quiescent counterparts of the neutron-star X-ray transient X1732-304.

## 2 OBSERVATIONS AND ANALYSIS

Terzan 1 was observed with the *Chandra X-ray Observatory* for  $\sim 19$  ks on 2005 May 10. The observation was made with the Advanced CCD Imaging Spectrometer (ACIS) with the telescope aim point on the back-illuminated S3 chip, this increases the sensitivity to low energy X-rays compared to the front-illuminated chips. Data reduction was performed using the CIAO v3.2.2 software with the calibration database CALDB v3.1.0, provided by the *Chandra* X-ray Center and

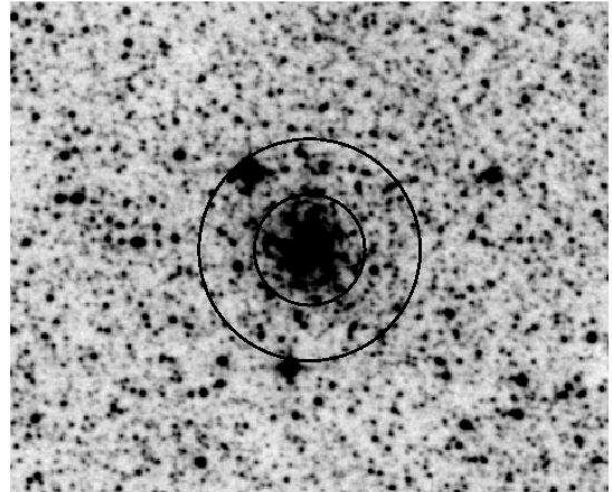


**Figure 1.** Digitized Sky Survey (DSS) image of Terzan 1. This IR plate was originally taken with the UK Schmidt Telescope. The inner circle indicates a radius of  $0.7'$  and the outer circle indicates a radius of  $1.4'$ .

following the science threads listed on the CIAO website<sup>1</sup>. No background flares were found, so all available data was used in our analysis. We removed the pixel randomisation added in the standard data processing as this slightly increases the spatial resolution of the images.

### 2.1 Source Detection

The CIAO tool `wavdetect` (Freeman et al. 2002) was used to detect the sources. We detected the sources in the 0.5-8.0 keV energy band. A detection threshold was chosen to give  $\sim 1$  false source over the S3 chip. We detect 39 sources over the entire S3 chip with 4 detected counts or greater, after the addition of one extra source close to the cluster centre. To get a good balance between including most of the cluster sources and minimising the number of nearby objects or background AGN it is standard in globular cluster studies to analyse the sources that are within the cluster half-mass radius. Trager et al. (1995) define the half-mass radius for this cluster to be 3.82 arcmin, however, they note that their measurement of this value is ‘particularly unreliable’. As this value for the half-mass radius is particularly large, and given that the majority of X-ray binaries in the cluster will be concentrated at the centre we chose a smaller region of size  $1.4'$  within which to analyse the X-ray sources (Fig. 1 shows a DSS image of Terzan 1). Within this  $1.4'$  region we find 14 sources. The *Chandra* image of the cluster is shown in Fig. 2 where all sources within the  $1.4'$  region are highlighted. These sources are listed in descending number of detected counts in Table 1, also included in this table is a list of sources on the S3 chip that are not within  $1.4'$  of the cluster center, listed in decreasing 0.5-8 keV counts. The position of the brightest source we detect, CX1, is consistent with the position of the source CXOGLB J173545.6-302900 from the previous *Chandra* HRC-I observation of Terzan

<sup>1</sup> Available at <http://cxc.harvard.edu/ciao/>.

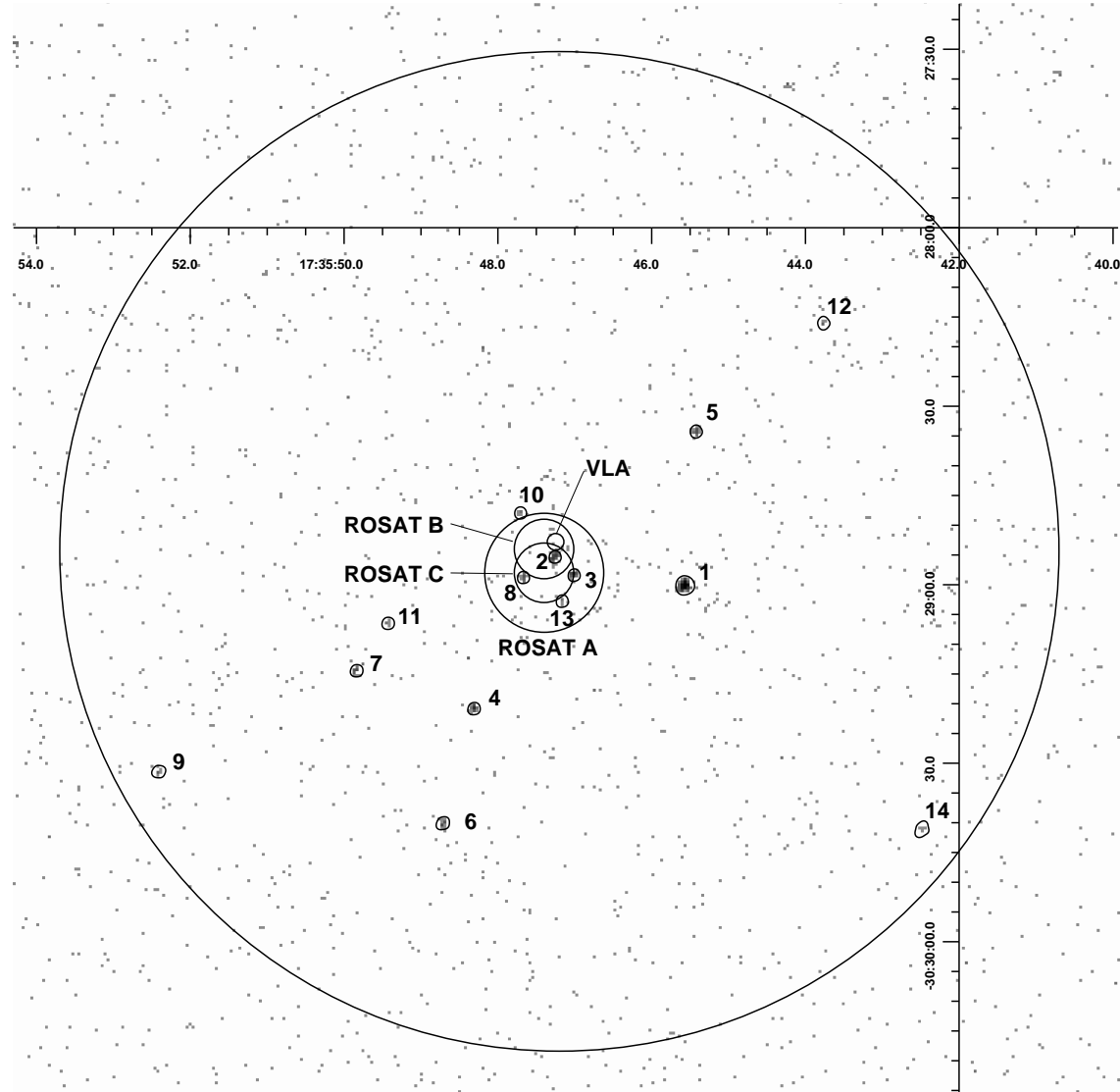


**Figure 2.** *Chandra* ACIS-S image of the globular cluster Terzan 1 in the 0.5-8.0 keV energy band. The large outer circle represents the 1.4' region within which we analyse the sources. The 14 sources within this region are labelled (in order of decreasing counts in the 0.5-8.0 keV band) and the extraction regions overlaid. Also shown are the *ROSAT* 1 $\sigma$  error circles for three pointings (see Johnston et al. 1995, for details), as well as the 1 $\sigma$  error circle of the radio source (using the error in declination as the radius, as this is largest) detected with the VLA (Marti et al. 1998). We predict that 2 of the detected sources are not associated with the cluster.

1 (Wijnands et al. 2002). From the density of sources on the S3 chip outside of the 1.4' region, we expect to find 2.2 sources not associated with the cluster (background or foreground objects) within the 1.4' region (assuming the sources outside this region are not associated with the cluster). This is in approximate agreement with the  $\log N - \log S$  relationships of Giacconi et al. (2001). Thus we expect that 2 of the 14 sources we detect within 1.4' are background or foreground sources.

## 2.2 Source Extraction

The IDL tool ACIS Extract (Broos et al. 2002) was used for source photometry and extraction of spectra. ACIS Extract makes use of CIAO, FTOOLS, ds9 display capability, and the TARA IDL software. ACIS Extract constructs polygon

source extraction regions which are approximate contours of the ACIS point-spread function (PSF). The user specifies the fraction of the PSF to be enclosed by the contour. The shape of the PSF at the location of each source is calculated using the CIAO tool *mkpsf*. For all our sources, except one, the PSF fraction contour level was set to 90%, evaluated at 1.5 keV. For the brightest source the PSF fraction was increased to 95%. With the chosen contour levels there is no overlapping of source extraction regions.

For each source spectra, light curves and event lists were extracted. The response matrix (RMF) and auxiliary response (ARF) files for each source are constructed using the CIAO tools *mkacisrmf* and *mkarf*. Background subtracted photometry was computed for each source in several different energy bands: 0.5-1.5 keV ( $X_{\text{soft}}$ ), 0.5-4.5 keV ( $X_{\text{med}}$ ), and 1.5-6.0 keV ( $X_{\text{hard}}$ ). These energy bands were chosen to

**Table 1.** Names, positions (J2000), and background-subtracted counts in four X-ray energy bands are given for the 14 sources detected within 1/4 of the center of Terzan 1 and the sources detected on the rest of the S3 chip. The count extraction region for each source within the 1/4 region is shown in Fig. 2. The source CX1 was first detected (and named) by Wijnands et al. (2002).

Source Name (Label) (1)	R.A. (h m s) (2)	Dec. (° ' '') (3)	0.5 - 8.0 keV (4)	0.5 - 1.5 keV (5)	0.5 - 4.5 keV (6)	Net Counts 1.5 - 6.0 keV (7)
CXOGLB J173545.6-302900 (CX1)	17 35 45.57	-30 29 00.1	225 <sup>+16</sup> <sub>-15</sub>	10 <sup>+4</sup> <sub>-3</sub>	157 <sup>+14</sup> <sub>-13</sub>	189 <sup>+15</sup> <sub>-14</sub>
CXOGLB J173547.2-302855 (CX2)	17 35 47.26	-30 28 55.3	43 <sup>+8</sup> <sub>-7</sub>	13 <sup>+5</sup> <sub>-4</sub>	38 <sup>+7</sup> <sub>-6</sub>	29 <sup>+7</sup> <sub>-5</sub>
CXOGLB J173547.0-302858 (CX3)	17 35 47.02	-30 28 58.4	31 <sup>+7</sup> <sub>-6</sub>	15 <sup>+5</sup> <sub>-4</sub>	31 <sup>+7</sup> <sub>-6</sub>	16 <sup>+5</sup> <sub>-4</sub>
CXOGLB J173548.3-302920 (CX4)	17 35 48.31	-30 29 20.8	29 <sup>+6</sup> <sub>-5</sub>	27 <sup>+6</sup> <sub>-5</sub>	28 <sup>+6</sup> <sub>-5</sub>	1 <sup>+2</sup> <sub>-1</sub>
CXOGLB J173545.4-302834 (CX5)	17 35 45.42	-30 28 34.2	19 <sup>+5</sup> <sub>-4</sub>	3 <sup>+3</sup> <sub>-2</sub>	17 <sup>+5</sup> <sub>-4</sub>	15 <sup>+5</sup> <sub>-4</sub>
CXOGLB J173548.7-302940 (CX6)	17 35 48.71	-30 29 40.0	17 <sup>+5</sup> <sub>-4</sub>	0 <sup>+2</sup>	11 <sup>+4</sup> <sub>-3</sub>	15 <sup>+5</sup> <sub>-4</sub>
CXOGLB J173549.8-302914 (CX7)	17 35 49.84	-30 29 14.4	16 <sup>+5</sup> <sub>-4</sub>	1 <sup>+2</sup> <sub>-1</sub>	13 <sup>+5</sup> <sub>-4</sub>	15 <sup>+5</sup> <sub>-4</sub>
CXOGLB J173547.6-302858 (CX8)	17 35 47.67	-30 28 58.7	15 <sup>+5</sup> <sub>-4</sub>	1 <sup>+2</sup> <sub>-1</sub>	13 <sup>+5</sup> <sub>-4</sub>	14 <sup>+5</sup> <sub>-4</sub>
CXOGLB J173552.4-302931 (CX9)	17 35 52.41	-30 29 31.3	7 <sup>+4</sup> <sub>-3</sub>	0 <sup>+2</sup>	7 <sup>+4</sup> <sub>-3</sub>	7 <sup>+4</sup> <sub>-3</sub>
CXOGLB J173547.7-302847 (CX10)	17 35 47.71	-30 28 47.9	6 <sup>+4</sup> <sub>-2</sub>	1 <sup>+2</sup> <sub>-1</sub>	5 <sup>+3</sup> <sub>-2</sub>	4 <sup>+3</sup> <sub>-2</sub>
CXOGLB J173549.4-302906 (CX11)	17 35 49.42	-30 29 06.4	5 <sup>+3</sup> <sub>-2</sub>	1 <sup>+2</sup> <sub>-1</sub>	4 <sup>+3</sup> <sub>-2</sub>	3 <sup>+3</sup> <sub>-2</sub>
CXOGLB J173543.7-302816 (CX12)	17 35 43.77	-30 28 16.0	5 <sup>+3</sup> <sub>-2</sub>	1 <sup>+2</sup> <sub>-1</sub>	5 <sup>+3</sup> <sub>-2</sub>	4 <sup>+3</sup> <sub>-2</sub>
CXOGLB J173547.1-302902 (CX13)	17 35 47.17	-30 29 02.7	4 <sup>+3</sup> <sub>-2</sub>	0 <sup>+2</sup>	4 <sup>+3</sup> <sub>-2</sub>	4 <sup>+3</sup> <sub>-2</sub>
CXOGLB J173542.4-302941 (CX14)	17 35 42.49	-30 29 41.0	4 <sup>+3</sup> <sub>-2</sub>	1 <sup>+2</sup> <sub>-1</sub>	4 <sup>+3</sup> <sub>-2</sub>	3 <sup>+3</sup> <sub>-2</sub>
Sources likely not associated with Terzan 1:						
CXOU J173538.1-303032	17 35 38.13	-30 30 32.1	128 <sup>+12</sup> <sub>-11</sub>	2 <sup>+3</sup> <sub>-1</sub>	100 <sup>+11</sup> <sub>-10</sub>	121 <sup>+12</sup> <sub>-11</sub>
CXOU J173548.1-303420	17 35 48.13	-30 34 20.2	74 <sup>+10</sup> <sub>-9</sub>	66 <sup>+9</sup> <sub>-8</sub>	73 <sup>+10</sup> <sub>-9</sub>	8 <sup>+4</sup> <sub>-3</sub>
CXOU J173553.1-303433	17 35 53.12	-30 34 33.2	56 <sup>+9</sup> <sub>-8</sub>	46 <sup>+8</sup> <sub>-7</sub>	57 <sup>+9</sup> <sub>-8</sub>	10 <sup>+5</sup> <sub>-3</sub>
CXOU J173545.6-303204	17 35 45.61	-30 32 04.9	45 <sup>+8</sup> <sub>-7</sub>	37 <sup>+7</sup> <sub>-6</sub>	44 <sup>+8</sup> <sub>-7</sub>	8 <sup>+4</sup> <sub>-3</sub>
CXOU J173536.4-302917	17 35 36.49	-30 29 17.9	31 <sup>+7</sup> <sub>-6</sub>	5 <sup>+3</sup> <sub>-2</sub>	30 <sup>+7</sup> <sub>-5</sub>	26 <sup>+6</sup> <sub>-5</sub>
CXOU J173535.9-303143	17 35 35.94	-30 31 43.4	30 <sup>+7</sup> <sub>-6</sub>	2 <sup>+3</sup> <sub>-1</sub>	21 <sup>+6</sup> <sub>-5</sub>	25 <sup>+6</sup> <sub>-5</sub>
CXOU J173547.1-303426	17 35 47.16	-30 34 26.1	27 <sup>+7</sup> <sub>-5</sub>	7 <sup>+4</sup> <sub>-3</sub>	24 <sup>+6</sup> <sub>-5</sub>	21 <sup>+6</sup> <sub>-5</sub>
CXOU J173557.2-302839	17 35 57.27	-30 28 39.2	19 <sup>+5</sup> <sub>-4</sub>	3 <sup>+3</sup> <sub>-2</sub>	15 <sup>+5</sup> <sub>-4</sub>	15 <sup>+5</sup> <sub>-4</sub>
CXOU J173559.8-303016	17 35 59.88	-30 30 16.8	17 <sup>+5</sup> <sub>-4</sub>	5 <sup>+3</sup> <sub>-2</sub>	17 <sup>+5</sup> <sub>-4</sub>	12 <sup>+5</sup> <sub>-3</sub>
CXOU J173547.7-303332	17 35 45.78	-30 33 32.5	17 <sup>+5</sup> <sub>-4</sub>	1 <sup>+2</sup> <sub>-1</sub>	12 <sup>+5</sup> <sub>-4</sub>	14 <sup>+5</sup> <sub>-4</sub>
CXOU J173534.2-302715	17 35 34.28	-30 27 15.3	13 <sup>+5</sup> <sub>-4</sub>	1 <sup>+2</sup> <sub>-1</sub>	10 <sup>+4</sup> <sub>-3</sub>	11 <sup>+4</sup> <sub>-3</sub>
CXOU J173533.7-303002	17 35 33.79	-30 30 02.5	13 <sup>+5</sup> <sub>-4</sub>	1 <sup>+2</sup> <sub>-1</sub>	7 <sup>+4</sup> <sub>-3</sub>	8 <sup>+4</sup> <sub>-3</sub>
CXOU J173556.0-302717	17 35 56.00	-30 27 17.3	12 <sup>+5</sup> <sub>-4</sub>	1 <sup>+2</sup> <sub>-1</sub>	7 <sup>+4</sup> <sub>-3</sub>	10 <sup>+4</sup> <sub>-3</sub>
CXOU J173550.1-303155	17 35 50.10	-30 31 55.0	9 <sup>+4</sup> <sub>-3</sub>	3 <sup>+3</sup> <sub>-2</sub>	10 <sup>+4</sup> <sub>-3</sub>	7 <sup>+4</sup> <sub>-3</sub>
CXOU J173554.2-302728	17 35 54.28	-30 27 28.8	8 <sup>+4</sup> <sub>-3</sub>	0 <sup>+2</sup>	8 <sup>+4</sup> <sub>-3</sub>	8 <sup>+4</sup> <sub>-3</sub>
CXOU J173544.2-302736	17 35 44.22	-30 27 36.2	8 <sup>+4</sup> <sub>-3</sub>	6 <sup>+4</sup> <sub>-2</sub>	8 <sup>+4</sup> <sub>-3</sub>	2 <sup>+3</sup> <sub>-1</sub>
CXOU J173603.7-302849	17 36 03.72	-30 28 49.9	8 <sup>+4</sup> <sub>-3</sub>	3 <sup>+3</sup> <sub>-2</sub>	8 <sup>+4</sup> <sub>-3</sub>	4 <sup>+3</sup> <sub>-2</sub>
CXOU J173544.0-303134	17 35 44.07	-30 31 34.8	8 <sup>+4</sup> <sub>-3</sub>	2 <sup>+3</sup> <sub>-1</sub>	5 <sup>+3</sup> <sub>-2</sub>	5 <sup>+3</sup> <sub>-2</sub>
CXOU J173602.1-303225	17 36 02.11	-30 32 25.0	7 <sup>+4</sup> <sub>-3</sub>	0 <sup>+2</sup>	7 <sup>+4</sup> <sub>-3</sub>	8 <sup>+4</sup> <sub>-3</sub>
CXOU J173535.9-302650	17 35 35.91	-30 26 50.9	7 <sup>+4</sup> <sub>-3</sub>	1 <sup>+2</sup> <sub>-1</sub>	6 <sup>+3</sup> <sub>-2</sub>	6 <sup>+4</sup> <sub>-2</sub>
CXOU J173539.7-303007	17 35 39.77	-30 30 07.0	6 <sup>+4</sup> <sub>-2</sub>	0 <sup>+2</sup>	4 <sup>+3</sup> <sub>-2</sub>	5 <sup>+3</sup> <sub>-2</sub>
CXOU J173555.0-302721	17 35 55.05	-30 27 21.9	5 <sup>+3</sup> <sub>-2</sub>	1 <sup>+2</sup> <sub>-1</sub>	5 <sup>+3</sup> <sub>-2</sub>	4 <sup>+3</sup> <sub>-2</sub>
CXOU J173540.7-302734	17 35 40.72	-30 27 34.0	5 <sup>+3</sup> <sub>-2</sub>	0 <sup>+2</sup>	5 <sup>+3</sup> <sub>-2</sub>	5 <sup>+3</sup> <sub>-2</sub>
CXOU J173547.8-303039	17 35 47.85	-30 30 39.0	4 <sup>+3</sup> <sub>-2</sub>	4 <sup>+3</sup> <sub>-2</sub>	4 <sup>+3</sup> <sub>-2</sub>	0 <sup>+2</sup>
CXOU J173544.7-303125	17 35 44.76	-30 31 25.6	4 <sup>+3</sup> <sub>-2</sub>	1 <sup>+2</sup> <sub>-1</sub>	4 <sup>+3</sup> <sub>-2</sub>	3 <sup>+3</sup> <sub>-2</sub>

be consistent with previous globular cluster studies in the literature (e.g. Grindlay et al. 2001a,b; Pooley et al. 2002a,b; Heinke et al. 2003a,b,c, 2005; Bassa et al. 2004). Table 1 lists the counts in each of these bands for all the sources. From the counts in the X<sub>soft</sub>, X<sub>med</sub> and X<sub>hard</sub> bands we create an X-ray color magnitude diagram, plotting the logarithm of the number of counts in the X<sub>med</sub> band against the X-ray color, defined as Xcolor = 2.5 log X<sub>soft</sub>/X<sub>hard</sub> (Grindlay et al. 2001a,b; Pooley et al. 2002a,b; Heinke et al. 2003a,b,c, 2005, though we note that Pooley et al. do not use the factor of 2.5) (see Fig. 3). Photoelectric absorption

reduces the number of counts detected and hence effects the X-ray colors and magnitudes. To allow comparison with sources in other globular clusters this needs to be corrected for. However, it is important to note that absorption affects each source differently. We determine an approximate correction for the effects of absorption by investigating the drop in count rate due to absorption for 3 typical spectra: a 3 keV thermal bremsstrahlung, a 0.3 keV blackbody, and a power-law with photon index,  $\Gamma$  = 2. (e.g. Pooley et al. 2002a,b). Using PIMMS, we determine the factor by which the count rate lowers with the inclusion of photoelectric ab-

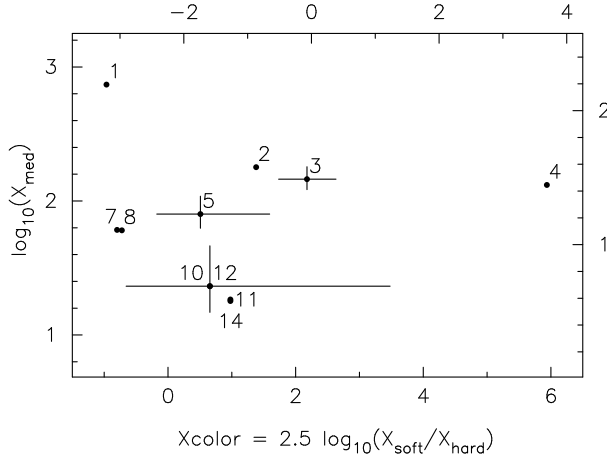


**Figure 3.** X-ray color magnitude diagram. The lower and left axes show the colors and magnitudes from the absorption-corrected counts, whilst the upper and right axes show the colors and magnitudes determined from the observed counts. We approximately correct for photoelectric absorption by shifting the data +0.69 units on the left axis and +2.25 units on the lower axis. Absorption affects each source differently, and our correction is only an approximation based on typical spectra of globular cluster sources. For the purposes of clarity, only a few error bars are shown. CX6, CX9 and CX13 are not shown as they have no counts in the  $X_{\text{soft}}$  band.

sorption at the column density seen for Terzan 1. The optical reddening,  $E(B-V) = 2.48 \pm 0.1$  (Ortolani et al. 1999), is converted to a column density  $N_H = 1.36 \times 10^{22} \text{ cm}^{-2}$  ( $N_H/E(B-V) = 5.5 \times 10^{21} \text{ cm}^{-2}$ , from Predehl & Schmitt 1995, using  $R = 3.1$ ). Absorption affects the  $X_{\text{soft}}$  band the most, with the absorbed count rate a factor of 13.92 lower on average for the three models. The other average correction factors are 4.85 for  $X_{\text{med}}$  and 1.76 for the  $X_{\text{hard}}$ . There is not a significant difference in the correction factors for the different models. This leads to a shift in  $X_{\text{color}}$  of +2.25 and a shift in  $\log X_{\text{med}}$  of +0.69. The lower and left axes of Fig. 3 show the absorption corrected colors and magnitudes, where as the upper and right axes show the observed values.

### 2.3 Spectral Analysis

Using XSPEC (v. 11.3.2) (Arnaud 1996) we fit the four brightest sources (CX1 - CX4) within the  $1.4'$  region. We attempt to fit each of the sources with 3 different models: the neutron star atmosphere model of Zavlin et al. (1996), a thermal bremsstrahlung model and a simple power-law. We both fix the column density at the cluster value ( $N_H = 1.36 \times 10^{22} \text{ cm}^{-2}$ ) and allow it to be free, using the photoelectric absorption model `phabs`. Errors in the fluxes were calculated by fixing the free-parameters to their maximum and minimum value in turn, and only one at a time. The model was then re-fitted to the data and flux values calculated. Once this was done for every free parameter, the flux range was used to give the flux errors.

We discuss each of these sources below. Table 2 gives the luminosities of the Terzan 1 sources as determined by spectral fits for CX1-3 assuming a distance to the cluster of 5.2 kpc. The luminosities for the other sources are de-

**Table 2.** Luminosities for X-ray sources in Terzan 1. For CX1-CX3 the luminosities have been calculated from the spectral fits (see text). For the other sources, PIMMS was used to estimate the fluxes from the detected source counts, assuming the cluster  $N_H$  and a power-law with  $\Gamma = 2.0$ . No luminosity is given for CX4 as it is possibly a foreground object.

Source	X-ray Luminosity ( $\text{ergs s}^{-1}$ )	
	0.5-2.5 keV	0.5-10 keV
CX1	$0.5^{+1.7}_{-0.3} \times 10^{33}$	$2.0^{+1.8}_{-0.3} \times 10^{33}$
CX2	$1.9^{+1.3}_{-0.7} \times 10^{32}$	$2.6^{+1.1}_{-0.5} \times 10^{32}$
CX3	$4.3^{+5.8}_{-2.4} \times 10^{32}$	$4.5^{+5.7}_{-2.1} \times 10^{32}$
CX5	$4.9 \pm 1.6 \times 10^{31}$	$8.5^{+2.4}_{-2.0} \times 10^{31}$
CX6	$8.1^{+11.7}_{-5.5} \times 10^{30}$	$7.6^{+2.4}_{-1.9} \times 10^{31}$
CX7	$2.1^{+1.5}_{-0.9} \times 10^{31}$	$7.2^{+2.3}_{-1.8} \times 10^{31}$
CX8	$1.3^{+1.2}_{-0.7} \times 10^{31}$	$6.7^{+2.3}_{-1.7} \times 10^{31}$
CX9	$1.7^{+1.4}_{-0.8} \times 10^{31}$	$3.1^{+1.7}_{-1.2} \times 10^{31}$
CX10	$3.9^{+10.0}_{-3.6} \times 10^{30}$	$2.6^{+1.6}_{-1.1} \times 10^{31}$
CX11	$8.1^{+11.7}_{-5.5} \times 10^{30}$	$2.2^{+1.6}_{-1.2} \times 10^{31}$
CX12	$1.3^{+1.2}_{-0.7} \times 10^{31}$	$2.2^{+1.6}_{-1.5} \times 10^{31}$
CX13	$3.9^{+10.0}_{-3.6} \times 10^{30}$	$1.7^{+1.5}_{-0.9} \times 10^{31}$
CX14	$1.7^{+1.4}_{-0.8} \times 10^{31}$	$1.7^{+1.5}_{-0.9} \times 10^{31}$

termined by estimating the fluxes from the detected source counts using PIMMS, and assuming the cluster  $N_H$  and a power-law with  $\Gamma = 2.0$ . A power-law with  $\Gamma = 2.0$  corresponds to an absorption-corrected  $X_{\text{color}} \sim 0.6$ , which is consistent with the majority of these sources (see Fig. 3).

#### 2.3.1 CXOGLB J173545.6-302900 (CX1)

The background-subtracted spectrum was grouped to have a minimum of at least 15 counts per bin. Both the neutron star atmosphere model and thermal bremsstrahlung model do not fit the spectrum satisfactorily with either the cluster  $N_H$  or allowing it to be a free parameter. A power-law model, with absorption at the cluster value, fits with a photon index,  $\Gamma = 0.2 \pm 0.2$  and a reduced  $\chi^2_\nu = 0.92$  for 13 degrees of freedom (dof). Allowing the photoelectric absorption to be a free parameter leads to a fit with  $N_H = 2.4^{+1.8}_{-1.1} \times 10^{22} \text{ cm}^{-2}$ ,  $\Gamma = 0.7^{+0.7}_{-0.6}$ , and  $\chi^2_\nu = 0.82$  for 12 dof. The photon index of the source from these power-law fits is unusually hard for globular cluster sources, and from the X-ray color-magnitude diagram it can be seen that this is the hardest source in the cluster. Only a few known globular cluster sources have  $\Gamma < 1.0$  and most tend to have  $\Gamma > 1.5$ . An example of a globular cluster source that under some observing conditions could look like CX1 is the CV X9 in 47 Tuc (Heinke et al. 2005). This source has very strong soft X-ray emission (see Fig. 18 in Heinkel et al. 2005), due to oxygen lines. Above  $\sim 5$  keV it shows more flux than can be accounted for with simple bremsstrahlung or power-law models; possibly this is due to partial covering absorption. Observing this object only above 2 or 3 keV (for instance, if it was in Terzan 1 and heavily obscured) would give an effective photon index of  $\sim 0.3$ . Recently, Munoz et al. (2004) detected many X-ray sources in the Galactic Center that have hard spectra, with a median photon index  $\Gamma = 0.7$ , though many have  $\Gamma \leq 0$ . These authors suggest that most of the sources are intermediate polars. Intermediate polars

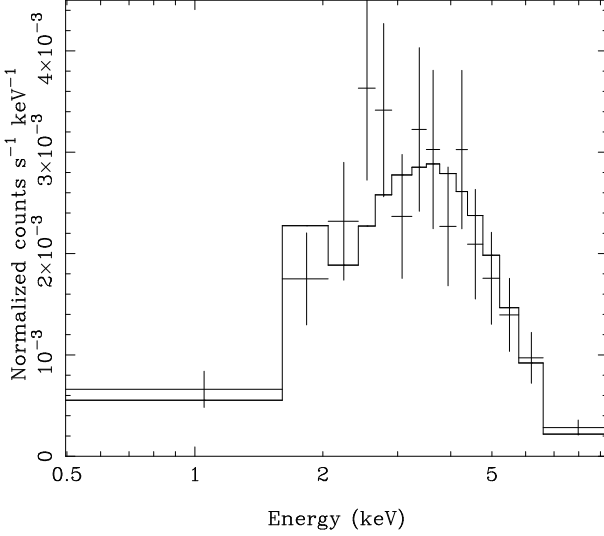


**Figure 4.** The spectrum of the brightest source in Terzan 1, CXOGLB J173545.6-302900 (CX1).

are more luminous and harder than other CVs. The hardness of these sources is thought to be due to local absorption (in addition to Galactic absorption) that is partially covering the X-ray emitting region, for example by material in the accretion flow. We therefore model CX1 absorbed by the average cluster absorption (using the `phabs` model, and fixing  $N_H = 1.36 \times 10^{22} \text{ cm}^{-2}$ ), plus an additional partially-covering absorption component that affects a fraction of the emitting region (using the `pcfabs` model). This leads to a fit with  $\chi^2_\nu = 0.78$  for 11 dof. This spectral fit is shown in Fig. 4. We get a higher photon index, with  $\Gamma = 1.1^{+1.0}_{-0.9}$ , with the partial absorption component having  $N_H = 3.4^{+3.8}_{-3.2} \times 10^{22} \text{ cm}^{-2}$  and a covering fraction of  $0.8^{+0.2}_{-0.6}$ . Thus, the partial covering absorption can explain the extreme hardness as the photon index has increased, and the source could be an intermediate polar. However, it is not possible to distinguish between the quality of these fits given the values of reduced  $\chi^2_\nu$ .

From this model we calculate the unabsorbed 0.5-2.5 keV luminosity  $= 0.5^{+1.7}_{-0.3} \times 10^{33} \text{ ergs s}^{-1}$  and the unabsorbed 0.5-10 keV luminosity  $= 2.0^{+1.8}_{-0.3} \times 10^{33} \text{ ergs s}^{-1}$  (assuming a distance of 5.2 kpc).

### 2.3.2 CXOGLB J173547.2-302855 (CX2)

As this source only has a total of 42.8 net counts in the 0.5-8 keV band, we did not group this spectrum into bins and cannot use  $\chi^2$  statistics. We therefore fit the spectrum in XSPEC using Cash statistics (Cash 1979) without subtracting a background spectrum (as Cash statistics cannot be used on background subtracted spectra). This should introduce a minimal error as there are only 0.2 background photons in the extraction region. To investigate the quality of fits, the ‘goodness’ command is used. This generates 10,000 Monte Carlo simulated spectra based on the model. If the model provides a good description of the data then approximately 50% of the simulations should have values of the Cash fit statistic that are lower than that of the best-fitting model. We define the fit quality as the fraction of the simulated

spectra with values of the Cash statistic lower than that of the data. Both very low and very high values of the fit quality indicate that the model is not a good representation of the data.

Fitting a neutron star atmosphere model to this spectrum (with the radius = 10 km, the mass =  $1.4 M_\odot$  and the normalisation =  $1/d(\text{pc})^2 = 3.7 \times 10^{-8}$ ) does not give a good fit, with a fit quality of 1.0. Fitting a thermal bremsstrahlung model also gives a reasonably poor fit, with a fit quality of 0.85. An improved fit is obtained when this spectrum is fitted with a simple power-law model at the cluster  $N_H$ , giving a photon index,  $\Gamma = 2.5 \pm 0.6$  and a fit quality of 0.65. Allowing the  $N_H$  to be a free parameter, gives  $N_H = 1.2^{+0.8}_{-0.6} \times 10^{22} \text{ cm}^{-2}$ ,  $\Gamma = 2.3 \pm 1.0$  and a fit quality of 0.7. Such a value of the photon index suggests that this could be a hybrid thermal plus power-law spectrum, but there are not enough counts to be conclusive. From the X-ray color-magnitude diagram we see that this source is relatively soft and so it is possible that it could be a quiescent neutron star X-ray binary. We determine a 0.5-2.5 keV luminosity of  $1.9^{+1.3}_{-0.7} \times 10^{32} \text{ ergs s}^{-1}$  and a 0.5-10 keV luminosity of  $2.6^{+1.1}_{-0.5} \times 10^{32} \text{ ergs s}^{-1}$  from the power-law fit with the cluster column density.

### 2.3.3 CXOGLB J173547.0-302858 (CX3)

This source also has too few counts to use  $\chi^2$  statistics and so we again use Cash statistics. A simple power-law fit at the cluster column density gives a photon index,  $\Gamma = 3.9 \pm 1.2$  and a fit quality of 0.51. Such a high photon index strongly suggests a soft thermal spectrum, which is also indicated by the X-ray color. A neutron star atmosphere fit (with the radius = 10 km, the mass =  $1.4 M_\odot$  and the normalisation =  $1/d(\text{pc})^2 = 3.7 \times 10^{-8}$ ) at the cluster column density gives  $T_{\text{eff}}^\infty = 73.7^{+3.3}_{-3.7} \text{ eV}$  with a fit quality of 0.65. Allowing the column density to be a free parameter does not greatly improve the fit, with  $N_H = 1.8^{+0.5}_{-0.4} \times 10^{22} \text{ cm}^{-2}$ ,  $T_{\text{eff}}^\infty = 78.9 \pm 6.7 \text{ eV}$  and a fit quality of 0.62. A thermal bremsstrahlung fit with the cluster column density gives  $kT = 0.6^{+0.6}_{-0.2} \text{ keV}$  with a fit quality of 0.68, where as with the column density left free we get  $N_H = 1.8^{+1.3}_{-0.9} \text{ cm}^{-2}$  and  $kT = 0.4^{+1.0}_{-0.2} \text{ keV}$  with a fit quality of 0.77. We determine a 0.5-2.5 keV luminosity of  $4.3^{+5.8}_{-2.4} \times 10^{32} \text{ ergs s}^{-1}$  and a 0.5-10 keV luminosity of  $4.5^{+5.7}_{-2.1} \times 10^{32} \text{ ergs s}^{-1}$  from the power-law fit with the cluster column density. From its spectrum, this source could be a quiescent neutron star.

### 2.3.4 CXOGLB J173548.3-302920 (CX4)

Cash statistics have also been used to analyse this source. This source is the softest source within the cluster, with an extremely high X-ray color. There is no valid power-law fit when fixing the column density to the cluster value. However, leaving this free we get a fit with  $N_H = 0.7^{+0.5}_{-0.6} \times 10^{22} \text{ cm}^{-2}$ ,  $\Gamma = 7.1^{+2.9}_{-4.3}$  and a fit quality of 0.74. There is no good fit for either a neutron star atmosphere model or a bremsstrahlung model. Such a soft X-ray color and spectrum, and the measured  $N_H$  being much lower than the cluster value suggest that this source may not be associated with the cluster and maybe a foreground object with a lower column density. However, there is no counterpart seen in the DSS or 2MASS images. As this could possibly

be a foreground object and the model is highly uncertain, we have not determined a luminosity for this source.

### 3 DISCUSSION

#### 3.1 The neutron-star X-ray transient X1732–304 in quiescence

The most likely candidate for the quiescent counterpart of the neutron-star X-ray transient X1732–304 is CX2. Of the 4 sources that are within the *ROSAT* error circles, it is the only one contained in all three (see Fig. 2, note that the 3 separate error circles are from the 3 separate *ROSAT* observations of the source). From the X-ray color-magnitude diagram we see that this source is relatively soft and its spectrum suggests that it could be a hybrid thermal plus power-law source. Thus, it is possible that it could be a quiescent neutron star X-ray binary. The fact that it cannot be fit with a power-law spectrum alone is consistent with what was found by Jonker et al. (2004); that the power-law fractional contribution increases for sources with luminosities decreasing from  $10^{33}$  erg s $^{-1}$  to  $10^{32}$  erg s $^{-1}$ . The position of CX2 is consistent with the position of 3 photons detected by Wijnands et al. (2002) and has a flux slightly lower than their predicted upper-limit. CX3 also has a suitably soft X-ray color and spectrum to be a possible candidate, however, its position is only consistent with two of the *ROSAT* pointings.

The source CX2 is also closest to, though not fully consistent with, the position of the radio source detected with the VLA which might be the radio counterpart of the transient. The position of this VLA source (RA:  $17^h35^m47.^s27$ , Dec:  $-30^\circ28'52.^s8$ ) is accurate to  $1.7''$  (90% confidence level radius, Marti et al. 1998), however, the phase calibrator for these VLA observations had calibrator code C, which could mean a maximum systematic error of  $0.^{\prime\prime}15$  (J. Marti, private communication). The offset between the radio and X-ray position is  $2.5''$ . The *Chandra* pointing accuracy is within the typical  $0.^{\prime\prime}6$  absolute astrometry (90% confidence level radius) (Aldcroft et al. 2000) as we find that the position of the X-ray source CXOGLB J173545.6-302900 (CX1) is consistent with the position of the same source in a previous *Chandra* observation of the cluster, with an offset of only  $0.^{\prime\prime}3$ . Given the uncertainties in the X-ray and particularly the radio position only a small systematic offset is required for the sources to be fully consistent.

For an additional check of the accuracy of the *Chandra* pointing, possible optical and infra-red counterparts were searched for. We searched for USNO-B1.0 (Monet et al. 2003) point sources that are close to ACIS Extract positions for the X-ray sources on the S3 chip. From this we get 3 optical sources that match the X-ray positions to within the  $0.^{\prime\prime}6$  absolute astrometry (90% confidence level radius) for *Chandra* (Aldcroft et al. 2000). These sources are CXOU J173544.2-302736, CXOU J173545.6-303204 and CXOU J173536.4-302917 and have offsets of  $0.^{\prime\prime}07$ ,  $0.^{\prime\prime}39$ , and  $0.^{\prime\prime}54$  respectively. The corresponding USNO-B1.0 sources are 0594-0571302, 0595-0586465, and 0594-0571303 which have positional accuracies of  $0.^{\prime\prime}2$ ,  $0.^{\prime\prime}1$ ,  $0.^{\prime\prime}4$  respectively (averaging the error in R.A. and Dec.). Matches with the 2MASS All-Sky Catalog of Point Sources (Cutri et al. 2003)

were also searched for. Of the USNO-B1.0 matched sources, CXOU J173545.6-303204 is the only one to match a 2MASS source, with an offset of  $0.^{\prime\prime}58$ . CXOU J173550.1-303155 also has a possible 2MASS counterpart, with an offset of  $0.^{\prime\prime}57$ . The possible optical (USNO-B1.0) counterpart for this source has an offset of  $0.^{\prime\prime}78$ . To check how many accidental matches we get, we apply a random offset of up to  $20''$  and count the number of matches (sources found to be within  $0.^{\prime\prime}6$  of each other). This was repeated 1000 times and the number of mean accidental matches of X-ray sources with the USNO-B1.0 catalogue was found to be  $0.2 \pm 0.5$ . The 3 sources we find is significantly above this mean.

As the radio source is not seen to be fully consistent with any X-ray source there is the possibility that it is an unrelated source, for example a background AGN or quasar, in which case the radio source would likely still be present and any future radio observation might prove this. It is also possible that we may not have detected X1732–304 in quiescence. Only one photon is detected in the 0.5-8 keV band within the VLA error circle, which could very likely be a background photon. Assuming fewer than 5 counts were detected in VLA error circle, this gives an upper limit on the count rate of  $2.7 \times 10^{-4}$  counts s $^{-1}$ . We use XSPEC to estimate an upper limit on the flux from this count rate. Initially we fix the parameters of an absorbed neutron star atmosphere model to the appropriate cluster values expect for the effective temperature. This parameter is then adjusted to match the required count rate of  $2.7 \times 10^{-4}$  counts s $^{-1}$ . The unabsorbed 0.5-10 keV luminosity upper limit is then determined to be  $8 \times 10^{31}$  ergs s $^{-1}$ . Such a luminosity is slightly lower than typically seen for quiescent neutron stars (e.g. Heinke et al. 2003c; Pooley et al. 2003) although this scenario cannot be ruled out.

Assuming that CX2 is the quiescent counterpart to X1732–304, it is possible to put limits on the length of time that the source will stay in quiescence. In the deep crustal heating model of quiescent neutron star emission (Brown et al. 1998) the quiescent luminosity depends on the time-averaged accretion rate of the source. Assuming standard core cooling, it is then possible to relate the quiescent flux,  $F_q$ , and the average flux during outburst,  $\langle F_o \rangle$ , with the average time the source is in outburst,  $t_o$ , and quiescence,  $t_q$ , via  $F_q \approx t_o/(t_o + t_q) \times \langle F_o \rangle / 135$  (e.g., Wijnands et al. 2001, 2002). We use the bolometric flux during outburst as estimated by Wijnands et al. (2002) to be  $1.5 \times 10^{-9}$  ergs cm $^{-2}$  s $^{-1}$ . To place upper limits on the thermal quiescent flux we use the neutron star atmosphere fit to the spectrum of CX2 with the column density at the cluster value. We fix the temperature to the upper limit from the fit and determine the bolometric flux (generating a dummy response from 0.001 - 100 keV and extrapolating the model). This gives  $F_q < 3.3 \times 10^{-13}$  ergs cm $^{-2}$  s $^{-1}$ . The outburst from X1732–304 was seen to last at least 12 yr, so, assuming that  $t_o = 12$  yr, we get  $t_q > 395$  yr. However, it is not clear how long the source was in outburst when it was first detected. If we assume that  $t_o = 17$  yr, then the lower limit for the quiescent time increases to  $t_q > 560$  yr. We note that the long outburst episode of this transient will have heated the crust significantly out of thermal equilibrium with the core and therefore the crust might still be cooling down toward equilibrium again. If that is the case, then the thermal flux related to the state of the core is even lower than the

measured value (hence the core is cooler) and the quiescent episode should be even longer to allow the core to cool down. We note that if CX2 is not the counterpart of the transient quiescent flux would be lower and therefore the predicted quiescent episodes would be even longer.

Disk-instability models suggest that such a long quiescent should not occur. During quiescence the disk will slowly fill up again and at some point, even a small change in mass transfer rate should trigger an outburst (e.g., Lasota 2001). Another neutron star X-ray transient observed to have been in outburst for  $>10$  yr is KS 1731-260. The quiescent flux of this neutron star also leads to the length of predicted quiescent episodes of several hundred years (Wijnands et al. 2001). However, the neutron star X-ray transient in the globular cluster NGC 6440 has much shorter outbursts and quiescent periods that are consistent with the observed quiescent flux (Cackett et al. 2005). Thus, it appears that for the quasi-persistent neutron stars X1732-304 and KS 1731-260 to be as cool as observed in quiescence either the quiescent periods are several hundreds of years long, or the quiescent periods are much shorter and enhanced neutrino cooling is required for the neutron star to cool more quickly. In the latter case it is possible that in these systems the neutron stars are relatively heavy as suggested by Colpi et al. (2001).

### 3.2 Comparison with other globular clusters

Pooley et al. (2003) found a relationship between the number of close binaries observed in X-rays in a globular cluster and the stellar encounter rate of the cluster (see their Figure 2). These authors calculate the stellar encounter rate by performing a volume integral of the encounter rate per unit volume,  $R \propto \rho^2/v$  (where  $\rho$  is the density and  $v$  is the velocity dispersion), out to the half-mass radius. This requires knowing the core density and velocity dispersion. Unfortunately, for Terzan 1 there are no measurements of the velocity dispersion available. Since  $\rho$  and  $v$  are constant over the core, we can estimate the encounter rate by  $\rho_0^{1.5} r_c^2$ . As Terzan 1 is a ‘core-collapse’ cluster and the core is not well-defined any estimate for the encounter rate based on core values will be unreliable. However, using the values for the core density,  $\rho_0$ , and core radius,  $r_c$ , from the Harris catalog (Harris 1996) we find that the core is a factor of 3.4 less dense than that of 47 Tuc and the core radius is a factor of 8 times smaller. We therefore estimate that the encounter rate of Terzan 1 will be a factor of  $3.4^{1.5} \times 8^2 \sim 400$  smaller than in 47 Tuc. Thus, based on the core density and core radius, the encounter rate for Terzan 1 is many tens to hundreds of times smaller than the value of 47 Tuc. As 47 Tuc has an encounter rate of 396 (in the (Pooley et al. 2003) normalisation), we estimate that Terzan 1 has an encounter rate of  $\sim 1$ .

Although this is only an estimate of the encounter rate in Terzan 1, it is clear that it is not expected to be large enough for the number of sources we detect in this cluster to be consistent with the Pooley et al. (2003) relationship between the number X-rays sources and the encounter rate. To account for the number of detected X-ray sources it may be that the cluster was previously much larger and that most of the stars have been lost, perhaps due to passages through the Galactic disk as was suggested for NGC 6397 by Pooley et al. (2003). This idea is supported by the fact

that Terzan 1 is in the bulge of the Galaxy and has the closest projection to the Galactic centre among known globular clusters. Further evidence for a previously more massive cluster comes from the spectroscopic study of Terzan 1 by Idiart et al. (2002). These authors identify apparent members of Terzan 1 with substantially higher metallicity and suggest that Terzan 1 may have captured these stars from the bulge during a previous epoch when the cluster was significantly more massive.

## 4 CONCLUSIONS

We have presented a  $\sim 19$  ks *Chandra* ACIS-S observation of the globular cluster Terzan 1. Within 1.4 arcmin of the cluster centre we detect 14 X-ray sources and predict that 2 of these are not associated with the cluster (background AGN or foreground objects). The brightest of these sources, CX1, is consistent with the position of CXOGLB J173545.6-302900 first observed during a short *Chandra* HRC-I observation of Terzan 1 (Wijnands et al. 2002). This source has a particularly hard spectrum for a globular cluster source, with a simple power-law fit giving a photon index of  $0.2 \pm 0.2$ . Such a hard spectrum suggests that this could be an intermediate polar (Muno et al. 2004). The position of the second brightest source, CXOGLB J173547.2-302855 (CX2), is the only source to have a position that is consistent with all 3 of the previous *ROSAT* pointings that observed the neutron star transient X1732-304 (Johnston et al. 1995). This source’s X-ray color and spectrum suggest that it could be a quiescent neutron star and therefore we find that this source is the most likely candidate for the quiescent counterpart of X1732-304. CX2 has a position closest to the position of the radio source detected in Terzan 1 by the VLA (Marti et al. 1998), though the positions are not fully consistent. Assuming standard core cooling, from the quiescent flux of CX2 we predict extremely long ( $>400$  yr) quiescent episodes of X1732-304, or enhanced core cooling, to allow the neutron star to cool. Having estimated the stellar encounter rate of this cluster we find significantly more sources than expected by the relationship of Pooley et al. (2003) perhaps because the cluster was previously much larger and that most of the stars have been lost due to passages through the Galactic disk.

## Acknowledgements

EMC gratefully acknowledges the support of a PPARC Studentship at the University of St Andrews. DP gratefully acknowledges support provided by NASA through Chandra Postdoctoral Fellowship grant PF4-50035 awarded by the Chandra X-ray Center, which is operated by the Smithsonian Astrophysical Observatory for NASA under contract NAS8-03060. The authors wish to thank P. Broos for his support with ACIS Extract.

This work makes use of the Digitized Sky Surveys which were produced at the Space Telescope Science Institute under U.S. Government grant NAG W-2166. This publication makes use of data products from the Two Micron All Sky Survey, which is a joint project of the University of Massachusetts and the Infrared Processing and Analysis Center/California Institute of Technology, funded

by the National Aeronautics and Space Administration and the National Science Foundation. This research has made use of the USNOFS Image and Catalogue Archive operated by the United States Naval Observatory, Flagstaff Station (<http://www.nofs.navy.mil/data/fchpix/>). This work has also made use of the VizieR online database of astronomical catalogues (Ochsenbein et al. 2000).

## REFERENCES

Aldcroft T. L., Karovska M., Cresitello-Dittmar M. L., Cameron R. A., Markevitch M. L., 2000, in Proc. SPIE Vol. 4012, p. 650-657, X-Ray Optics, Instruments, and Missions III, Joachim E. Truemper; Bernd Aschenbach; Eds. Initial performance of the aspect system on the Chandra Observatory: postfacto aspect reconstruction. pp 650-657

Arnaud K. A., 1996, in ASP Conf. Ser. 101: Astronomical Data Analysis Software and Systems V XSPEC: The First Ten Years. p. 17

Bassa C., Pooley D., Homer L., Verbunt F., Gaensler B. M., Lewin W. H. G., Anderson S. F., Margon B., Kaspi V. M., van der Klis M., 2004, *ApJ*, 609, 755

Borrel V., et al., 1996a, *A&AS*, 120, 249

Borrel V., et al., 1996b, *ApJ*, 462, 754

Broos P., Townsley L., Getman K., Bauer F., 2002, ACIS Extract, An ACIS Point Source Extraction Package. Pennsylvania State University

Brown E. F., Bildsten L., Rutledge R. E., 1998, *ApJ*, 504, L95

Cackett E. M., Wijnands R., Heinke C. O., Edmonds P. D., Lewin W. H. G., Pooley D., Grindlay J. E., Jonker P. G., Miller J. M., 2005, *ApJ*, 620, 922

Campana S., Colpi M., Mereghetti S., Stella L., Tavani M., 1998, *A&AR*, 8, 279

Campana S., Stella L., 2000, *ApJ*, 541, 849

Cash W., 1979, *ApJ*, 228, 939

Colpi M., Geppert U., Page D., Possenti A., 2001, *ApJ*, 548, L175

Cutri R. M., et al., 2003, VizieR Online Data Catalog, 2246

Freeman P. E., Kashyap V., Rosner R., Lamb D. Q., 2002, *ApJS*, 138, 185

Giacconi R., et al., 2001, *ApJ*, 551, 624

Grindlay J. E., Heinke C., Edmonds P. D., Murray S. S., 2001a, *Sci*, 292, 2290

Grindlay J. E., Heinke C. O., Edmonds P. D., Murray S. S., Cool A. M., 2001b, *ApJ*, 563, L53

Guainazzi M., Parmar A. N., Oosterbroek T., 1999, *A&A*, 349, 819

Harris W. E., 1996, *AJ*, 112, 1487

Heinke C. O., Edmonds P. D., Grindlay J. E., Lloyd D. A., Cohn H. N., Lugger P. M., 2003a, *ApJ*, 590, 809

Heinke C. O., Grindlay J. E., Edmonds P. D., Cohn H. N., Lugger P. M., Camilo F., Bogdanov S., Freire P. C., 2005, *ApJ*, 625, 796

Heinke C. O., Grindlay J. E., Edmonds P. D., Lloyd D. A., Murray S. S., Cohn H. N., Lugger P. M., 2003b, *ApJ*, 598, 516

Heinke C. O., Grindlay J. E., Lugger P. M., Cohn H. N., Edmonds P. D., Lloyd D. A., Cool A. M., 2003c, *ApJ*, 598, 501

Idiart T. P., Barbuy B., Perrin M.-N., Ortolani S., Bica E., Renzini A., 2002, *A&A*, 381, 472

Inoue H., Koyama K., Makishima K., Matsuoka M., Murakami T., Oda M., Ogawara Y., Ohashi T., Shibasaki N., Tanaka Y., 1981, *ApJ*, 250, L71

Johnston H. M., Verbunt F., Hasinger G., 1995, *A&A*, 298, L21

Jonker P. G., Galloway D. K., McClintock J. E., Buxton M., Garcia M., Murray S., 2004, *MNRAS*, 354, 666

Lasota J.-P., 2001, *New Astronomy Review*, 45, 449

Makishima K., et al., 1981, *ApJ*, 247, L23

Marti J., Mirabel I. F., Rodriguez L. F., Chaty S., 1998, *A&A*, 332, L45

Menou K., McClintock J. E., 2001, *ApJ*, 557, 304

Monet D. G., et al., 2003, *AJ*, 125, 984

Muno M. P., Arabadjis J. S., Baganoff F. K., Bautz M. W., Brandt W. N., Broos P. S., Feigelson E. D., Garmire G. P., Morris M. R., Ricker G. R., 2004, *ApJ*, 613, 1179

Ochsenbein F., Bauer P., Marcout J., 2000, *A&AS*, 143, 23

Ortolani S., Barbuy B., Bica E., Renzini A., Marconi G., Gilmozzi R., 1999, *A&A*, 350, 840

Parmar A. N., Stella L., Giommi P., 1989, *A&A*, 222, 96

Pavlinsky M., Grebenev S., Finogenov A., Sunyaev R., 1995, *Advances in Space Research*, 16, 95

Pooley D., et al., 2003, *ApJ*, 591, L131

Pooley D., Lewin W. H. G., Homer L., Verbunt F., Anderson S. F., Gaensler B. M., Margon B., Miller J. M., Fox D. W., Kaspi V. M., van der Klis M., 2002a, *ApJ*, 569, 405

Pooley D., Lewin W. H. G., Verbunt F., Homer L., Margon B., Gaensler B. M., Kaspi V. M., Miller J. M., Fox D. W., van der Klis M., 2002b, *ApJ*, 573, 184

Predehl P., Schmitt J. H. M. M., 1995, *A&A*, 293, 889

Skinner G. K., Willmore A. P., Eyles C. J., Bertram D., Church M. J., 1987, *Nat*, 330, 544

Stella L., Campana S., Colpi M., Mereghetti S., Tavani M., 1994, *ApJ*, 423, L47

Terzan A., 1966, *C.R. Acad. Sci. Ser. B1*, 263, 221

Trager S. C., King I. R., Djorgovski S., 1995, *AJ*, 109, 218

Verbunt F., Bunk W., Hasinger G., Johnston H. M., 1995, *A&A*, 300, 732

Warwick R. S., Norton A. J., Turner M. J. L., Watson M. G., Willingale R., 1988, *MNRAS*, 232, 551

Wijnands R., Heinke C. O., Grindlay J. E., 2002, *ApJ*, 572, 1002

Wijnands R., Miller J. M., Markwardt C., Lewin W. H. G., van der Klis M., 2001, *ApJ*, 560, L159

Zavlin V. E., Pavlov G. G., Shibanov Y. A., 1996, *A&A*, 315, 141